Nanopore translocation of topologically linked DNA catenanes

Sierra N. Rheaume 10

School of Physics, Georgia Institute of Technology, Atlanta, Georgia 30332, USA

Alexander R. Klotz • *

Department of Physics and Astronomy, California State University, Long Beach, Long Beach, California 90815, USA

(Received 1 September 2022; revised 9 January 2023; accepted 9 February 2023; published 27 February 2023)

The electrical signal associated with a biopolymer translocating through a nanoscale pore depends on the size, topology, and configuration of each molecule. Building upon recent interest in using solid-state nanopores for studying the topology of knotted and supercoiled DNA, we present experimental observations of topologically linked catenanes translocating through a solid-state nanopore. Using restriction enzymes, linked circular molecules were isolated from the mitochondrial DNA of Crithidia fasciculata, a structure known as a kinetoplast that comprises thousands of topologically interlocked minicircles. Digested kinetoplasts produce a spectrum of catenane topologies, which are identified from their nanopore translocation signals by spikes in the blockade current associated with the topological linkages. We attribute the different patterns of the measured electrical signals to 2-catenanes, linear and triangular 3-catenanes, and several types of 4- and 5-catenanes as well as more complex structures. Measurements of the translocation time of signals consistent with 2- and 3-catenanes suggest that topological friction between the linkages and the pore slows the translocation time of these structures, as predicted in recent simulations.

DOI: 10.1103/PhysRevE.107.024504

I. INTRODUCTION

Nanopore sensors detect the electrical current associated with the passage of an ionic fluid through a nanoscore pore in a membrane. Biomolecules translocating through the pore cause current blockades that may be used to detect or characterize the molecules [1]. Nanopore sequencing, in which the genetic sequence is reconstructed by using the current blockade associated with individual nucleotides, has recently become a viable tool for long-read-length sequencing using biological pores [2]. Solid-state nanopores offer greater versatility and tunability than biological pores, and have been used for identifying the binding of individual proteins bound to DNA [3] and for direct protein detection [4]. The development of nanopore technology has grown in step with an improved understanding of polymer dynamics during the translocation process [5,6]. Recently, there has been theoretical interest in the physics and rheology of topologically complex polymers, including rings [7], branched chains [8], knots [9], and catenanes [10]. Many of the experimental investigations have used DNA as a model system. Recently, experiments examining knotted DNA in solid-state nanopores have provided information about the frequency of stochastic knots in DNA [11], the size distribution of knots in DNA [12], and the mechanisms by which knots deform as they translocate [13]. While knots in linear strands are transient and can untie before or during translocation, linked-ring catenanes are topologically robust. Experiments with catenanes have the potential to explore so-called "topological friction" in a way that previous

experiments have not been able to. While there have been simulation studies of the catenane translocation process [14,15], experiments have been lacking.

Much of the interest in topologically complex translocation concerns topological friction, a phenomenon whereby the altered topology of a molecule influences its tribological interactions with its environment. Hypothesized to explain the ejection of knotted genomes from virus capsids [16], topological friction has been studied in the context of knot diffusivity [17] as well as the translocation of knotted DNA molecules through pores [18–20]. Experiments with knotted translocation have provided only transient data for topological friction [11]. In contrast, simulations of catenane translocation predict much stronger topological friction effects, including a jamming associated with the linkage between catenated rings that has a significant influence on the translocation time [14,15].

Kinetoplast DNA (kDNA), often described as "molecular chainmail," is a complex DNA structure consisting of several thousand linked circular molecules around 2500 base pairs in length, known as minicircles, and several dozen larger circular molecules called maxicircles, around 40 000 base pairs in length [21]. kDNA is found in the mitochondria of trypanosome parasites, which are responsible for diseases such as leishmaniasis, Chagas disease, and sleeping sickness. kDNA is part of a complex gene-editing apparatus that allows metabolic proteins to be expressed by modifying the mitochondrial messenger RNA [22]. Kinetoplast biology is an active area of parasitology research [23] and kDNA has recently been explored as a model system for two-dimensional polymer physics [24,25]. Here, we use kinetoplasts from Crithidia fasciculata as a source of topological linkages to

^{*}alex.klotz@csulb.edu

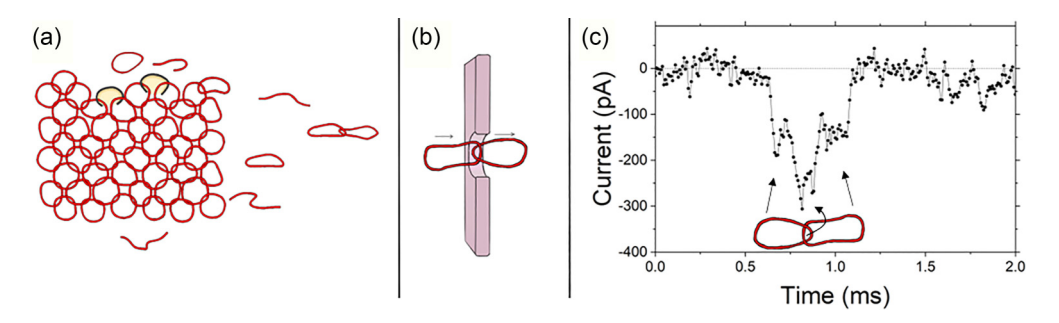


FIG. 1. (a) Schematic of kinetoplast DNA (red) being digested by XhoI restriction enzymes (yellow/black) which linearize molecules and can release isolated circles and catenanes from the network. (b) Schematic of a Hopf link or 2-catenane translocating through a pore. (c) The translocation current from an experiment showing two baseline drops connected by a deeper blockade, which we interpret as the linkage between two Hopf-linked minicircles.

investigate catenane translocation. Restriction enzymes can linearize minicircles within kinetoplast networks, which can release catenanes of various complexity into the solution [Fig. 1(a)] [26]. These released catenanes make up an ensemble of topologically diverse molecules that we can observe using a solid-state nanopore [Fig. 1(b)].

II. EXPERIMENTS

Kinetoplast DNA from *Crithidia fasciculata* (TopoGEN) was digested with XhoI restriction enzyme [schematic in Fig. 1(a)] in CutSmart buffer (New England BioLabs) in a 50 μ L aqueous solution containing 1 μ g of kDNA, 5 μ L of CutSmart buffer, and 1 μ L of XhoI at the supplier's stock solution. The solution was placed in a 37 °C water bath for up to 20 min. Proteinase K was added to the solution after the allotted time to suppress additional digestion. Following the results of Chen *et al.* [26], this produced a spectrum of topologically connected DNA molecules with a frequency that depends on the degree of enzyme digestion and the underlying connectivity of the kinetoplast network. The digested DNA solution was diluted in 4M lithium chloride solution to a molecular number density of approximately 1 nM.

Solid-state nanopores in silicon nitride membranes embedded in microfluidic *cis* and *trans* channels were enlarged using controlled dielectric breakdown [27] by filling the channels with 4M LiCl and applying 10 V across the membrane. The typical size of the nanopores is between 30 and 50 nm.

The NanoCounter (Ontera, Inc.) was used both to enlarge the nanopores and to facilitate and detect the translocation of DNA by applying a 100 mV potential difference across the pore and measuring the current through it [schematic in Fig. 1(b)]. Thousands of DNA translocation events were observed in each experiment, many of them containing short spikes of excess current blockage in the interior of the molecule. These spikes are similar to those observed in knotted molecules, reported in previous studies [11–13]. A characteristic molecular translocation signal associated with a Hopf link (2-catenane) can be seen in Fig. 1(c).

In order to determine the topology of translocating molecules, we predicted the translocation signal of each expected configuration with up to five catenated links [26], and used the SPIRaL classification scheme developed by Sharma et al. [12] to predict their translocation signal based on the number strands expected to occupy the pore as the molecule translocates. For example, a Hopf link is expected to have two strands in the pore as the first minicircle translocates, four as the linkage translocates, and two as the second translocates, and would have a SPIRaL code of 2-4-2, which is observed in Fig. 1(c). For structures that are not symmetric, we classified both orientations (e.g., 2-6-4 and 4-6-2 for a triangular 3-catenane) as the same topology. Similar to previous work used to classify knots, we examined the translocation signal of molecules that were localized above the median translocation time and mean current blockade, and classified them into their expected topologies. Figure 2 shows four of the

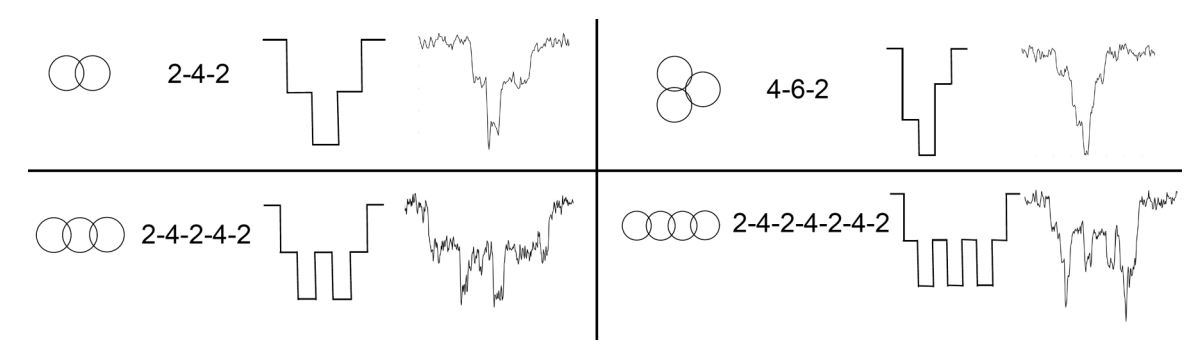


FIG. 2. Four of the simplest expected catenane topologies (2-catenanes, linear and triangular 3-catenanes, and the linear 4-catenane). Shown are a diagram of their topology, their predicted SPIRaL classification based on the number of concurrent DNA strands within the pore during translocation, a predicted translocation signal based on the SPIRaL classification, and an example of an observed signal.

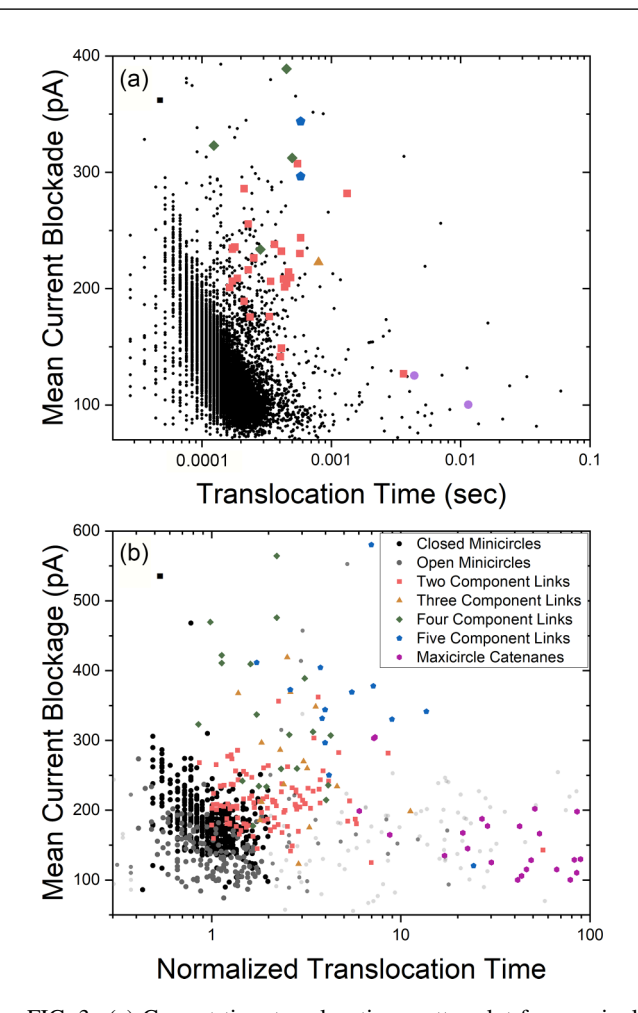


FIG. 3. (a) Current-time translocation scatter plot from a single experiment showing the open and closed minicircles in black and more complex interpreted topologies colored according to the legend in (b). The secondary cluster to the right of the main minicircle cluster likely contains cleaved maxicircle fragments. (b) Collected current-time scatter plot showing interpreted nontrivial minicircle topologies aggregated over several experiments, color coded according to the number of minicircles in the translocating structure. The gray and black data are from experiments with isolated linear and circular minicircles, with possibly spurious events from maxicircles or residual catenanes presented semitransparently. Translocation time data are normalized to the peak time of the (linear+circular) minicircle histogram.

simplest topologies, and a listing of all observed topologies, their SPIRaL classifications, predicted signals, and interpreted signal observations, can be seen in Fig. 6 in the Appendix, with unobserved topologies listed in Fig. 7. We observed signals consistent with the 2-catenane, both forms of the 3-catenane, three of five 4-catenanes, and six to seven of eleven 5-catenanes, as well as structures consistent with maxicircles linked to minicircles.

III. RESULTS AND DISCUSSION

Translocation statistics are visualized on a mean current blockade-versus-translocation time scatter plot. A plot from a single experiment can be seen in Fig. 3(a), where the majority of translocations lie in a banana-shaped region of constant

charge deficit, associated with single minicircles. This region contains an aggregate of both open and closed minicircles; molecules towards the bottom right are likely to be linear and molecules at the top left circular, but it is difficult to identify the topology of a single molecule. We observe a secondary region at slightly longer time which we associate with fragments from cleaved maxicircles. Compared to experiments with standard linear or circular molecules, we observe a significant population of translocations away from the banana. Observing these translocations suggests features associated with molecular catenanes, which we have examined, classified, and color coded by their interpreted topology in Figs. 3(a) and 3(b).

We are interested in the mean translocation time of exotic topologies, which is pore size dependent. The Ontera NanoCounter created pores through controlled dielectric breakdown, and produces a stochastic range of pore sizes compared to those created by electron or ion beam milling. In order to normalize experimental data recorded on different devices, we examine a histogram of linear and circular minicircle translocations for each experiment, find the peak to define a typical minicircle translocation time, and divide each exotic translocation time by the peak time for that experiment. Because the single-minicircle data are aggregates of both linear and circular molecules, the peak time is in between the peak time of linear and circular molecules, and the measured ratio of exotic topologies should be considered a lower bound on the ratio of each topology to a single minicircle.

An aggregated scatter plot in Fig. 3(b) shows normalized data from conventional (linear and circular) and exotic topologies. Although we cannot distinguish the topology of molecules in the single-minicircle data cloud in a typical experiment, we present data from experiments with closed and open minicircles as a basis of comparison for the catenane translocations. Samples of closed and open minicircles from topoisomerase and restriction enzyme reactions respectively are provided by TopoGen, although these samples contain maxicircles and possibly residual catenanes. The overlap between the top of the open minicircle point cloud and the bottom of the closed minicircle point cloud make it difficult to tell whether any individual translocation in that region of the scatter plot is linear or circular if not already known. The data in Fig. 3(b) show the normalized translocation times and mean currents of exotic translocations color coded according to their ascertained topology. Most of the observations we associate with catenanes were Hopf links, followed by linear and triangular 3-catenanes. We have observed a significant population of likely combined maxicircle-minicircle complexes. We have observations associated with nearly every expected topological structure of up to five minicircles at least once (but not in sufficient numbers for meaningful statistics). Generally speaking, we observed significantly fewer catenanes than predicted by the analysis of Chen et al. [26], who used gel electrophoresis. The intensity of a gel band is proportional to the mass of the DNA in the band rather than the number of distinct molecules; thus the larger catenanes are easier to detect compared to a nanopore experiment. In addition there may be differences in the nanopore capture process due to topology and as such, we refrain from making inferences based on the observed topological distribution. A natural follow-up would be to measure the translocations of DNA extracted from the

TABLE I. Ratios of the mean translocation time for 2-catenanes, linear 3-catenanes, and closed (triangular) 3-catenanes to the peak translocation time of linear and open minicircles, with standard error. Computational data from Carraglio and Orlandini [15,28] is provided as a comparison. Because the nanopore cannot distinguish between linear and closed minicircles, the measured ratios should be treated as a lower bound.

Topology	Expt. time ratio	Comput. time ratio [15,28]
2-catenane	2.7 ± 0.5	2.7
3-catenane	3.9 ± 1.1	4.8
Triangle	2.5 ± 0.3	4.0

gel bands of a Chen-type experiment. Unfortunately, we were unable to do so as the manufacturer of our nanopore amplifier and the nanopore chips, Ontera, Inc., ceased operations shortly after these experiments were completed. We intend to perform that assay with new equipment in the future.

The normalized mean translocation times events associated with of the three most common exotic topologies are found in Table I. As a point of comparison we show similar data from a simulation study [14,15] as well as unpublished data provided by the author [28] using the unknot translocation time as the basis of normalization. As the simulations use a smaller pore size and flexible (not semiflexible) chains, comparisons should be treated as qualitative. Due to being observed in a much greater quantity, we regard our 2-catenane results as being the most significant.

Arguments may be made that topological complexity can either speed up or slow down a molecule in tight confinement: a speed-up effect due to the effective shortening of the molecule due to a knot, or a slowing effect predicted to arise from topological friction. If topological friction dominates over shortening, we expect the 2-catenane to take more than twice as long to translocate as an isolated minicircle. Our observed ratio of 2.7 ± 0.5 indicates that topological friction is significant. The 3-catenane is expected to take more than 1.5 times that of the 2-catenane to translocate if friction dominates, although our data are not precise enough to make that observation. The shorter translocation of triangles compared to linear 3-catenanes indicates that shortening can also be a significant effect, similar to the shorter translocation times for

knotted DNA seen in previous experiments [11,12]. There are additional factors that affect the translocation time of linked molecules: Because the electric field is strongest within the pore, the forward motive force on the molecule is greater when the linkage, with greater volumetric charge density, is within the pore. While the slow speed of the Hopf link may indicate that friction within the pore dominates, the comparatively fast speed of the triangular catenane may be indicative of competing motive and friction effects. Another comparison may be made between Hopf links and single loops with twice the contour length, although a direct comparison is difficult because of the superlinear translocation time exponent [29,30]. Hopf links are predicted to translocate slightly faster than doublesized single links [15] due to a balance of friction, shortening, and length-dependence effects, a phenomenon that can be clarified in a future experiment.

One of the predictions of Caraglio and Orlandini is that topological friction causes the linkage between molecules to dwell in the pore for long periods of time [14,15]. This would manifest itself experimentally as an extended drop in the measured current. Figure 4(a) shows several 2-catenane translocations with a broad distribution of linkage spike widths is observed. Many are short, but several last for a time comparable to the translocation of a complete minicircle, suggesting that jamming effects are present. We measured the linkage translocation time by counting the number of contiguous time points in each molecule the translocation signal was below a threshold of 1.5 times the median current blockade level. A histogram of the linkage translocation time is shown in Fig. 4(b), with a peak at short times but a broad tail with a few observed long outliers. This lends further support to our assertion that the linkage between two linked minicircles experiences topological friction within the pore.

The distribution of timescales of the first and second loop blockades, as well as that of the linker blockade, are presented in Fig. 5 and contain information about the dynamics of the translocation process. In studies of the translocation of knotted circular DNA, for example, the highly skewed distribution of the time of the blockade minimum is indicative that the knot slides as it translocates. We do not observe a significant bias: The point during the translocation at which the current is minimized is found at 0.52 ± 0.01 relative to the translocation of the entire molecule. The average relative

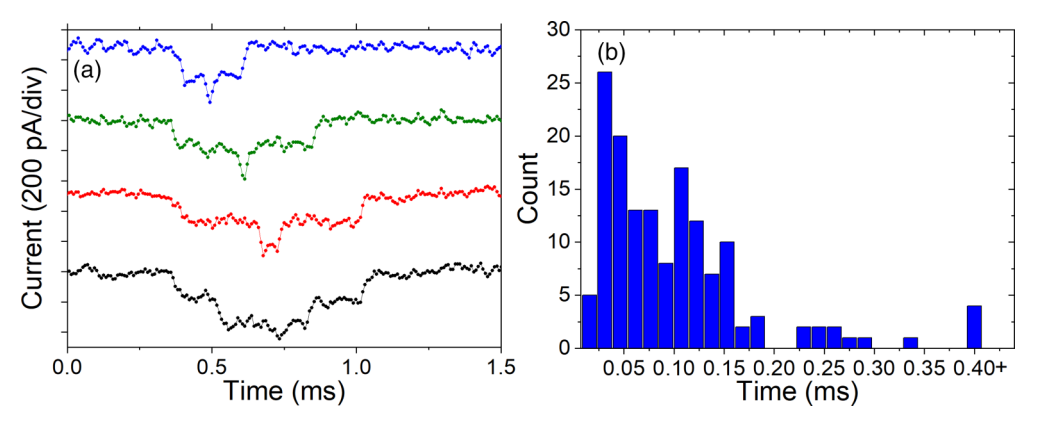


FIG. 4. (a) Several current trace translocations interpreted as 2-catenanes or molecular Hopf links. Variation can be seen in the width of the central spike. (b) Histogram of observed spike distribution times for the population of translocating 2-catenanes.

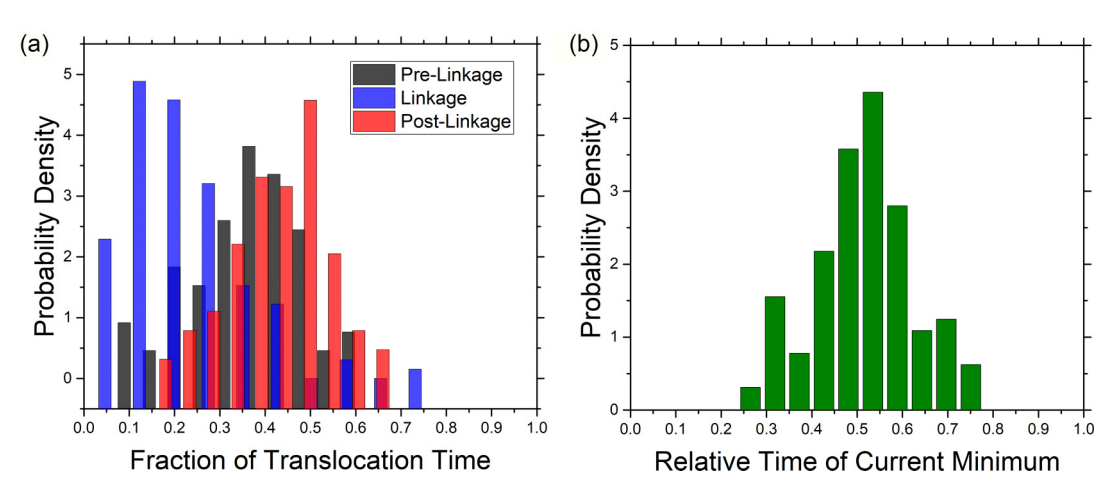


FIG. 5. Histograms of (a) the relative times of the translocation before, during, and after the linkage and (b) the location of the current minimum for 2-catenane events. The pre- and postlinkage data in (a) are not significantly different, and the location of the current minimum is evenly distributed around the halfway point.

translocation time of the first loop before the linkage is 0.40 ± 0.01 and the second loop after the linkage is 0.38 ± 0.01 . A greater translocation speed towards the end of the molecule after a topological event was predicted in simulations by Suma and Micheletti [30] due to a transition between tension

propagation and tail retraction. Due to our comparatively larger pores reducing the effect of tension propagation, and the lack of knot sliding, the small difference in pre- and postlink translocation times we observe does not contradict those simulations.

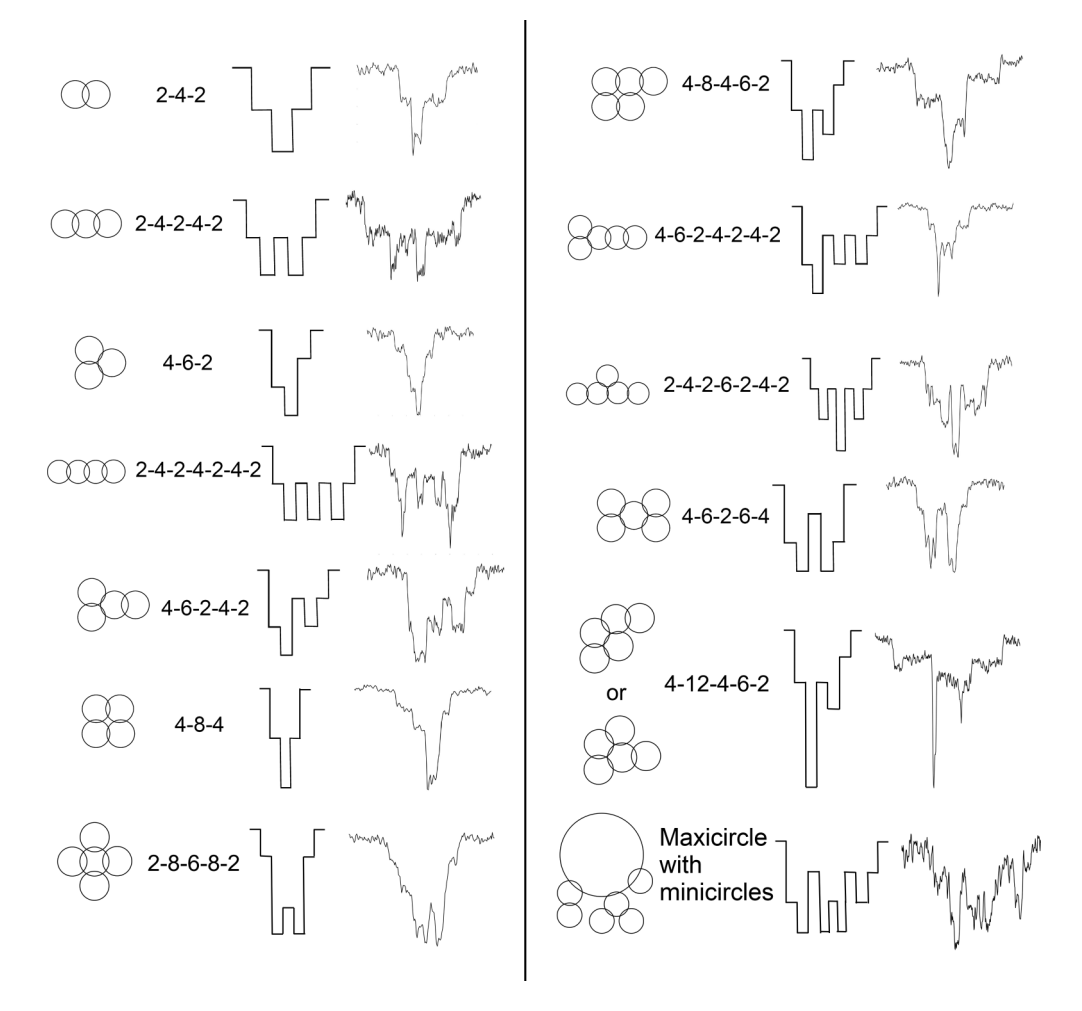


FIG. 6. Table of linked topologies, their SPIRaL classification [12], a schematic of a translocation, and an observed translocation. The final topology likely includes a maxicircle linked to several minicircles, with unknown exact topology.

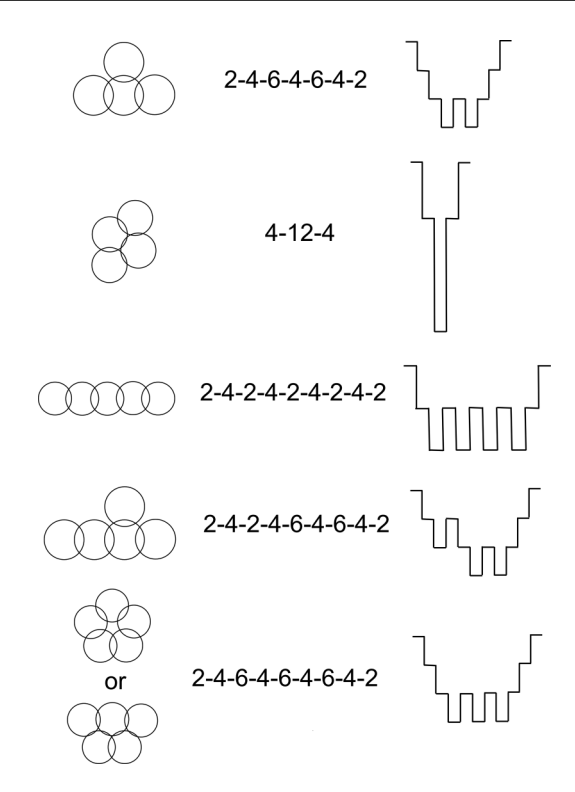


FIG. 7. Catenated structures, their SPIRaL classification, and predicted translocation structure, for topologies that were not observed.

IV. CONCLUSION

We used a solid-state nanopore to study the translocation signature of DNA catenanes, isolated from kinetoplasts using restriction enzymes. We associate the different patterns of the measured electrical signals to a rich spectrum of topological structures. The topology dependence of the translocation time of these catenanes indicates the presence of topological friction between the linkages and the pore, as predicted by simulations. This study used pores that were up to 12 times larger in diameter than the minimum width of circular DNA: Future experiments may probe translocation in sub-10-nm pores comparable to the minimum width of circular DNA molecules, and use topoisomerase decatenation rather than

restriction digestion to produce a broader spectrum of catenated topologies. Many simulation studies focus on increasingly exotic topological linkages between pairs of rings, but we hope this work inspires investigation into the translocation of more complex Hopf-linked rings [31], similar to those now observable experimentally.

ACKNOWLEDGMENTS

This work is supported by the National Science Foundation, Grant No. 2105113, as well as a CSUPERB New Investigator Award. S.N.R. was supported by a Google Summer Research Assistantship and an Edison STEM-NET Student Scholarship Award. The authors thank Enzo Orlandini for providing simulation data and insight, Natalie Fredriksson for assistance with the apparatus, as well as the anonymous referees for their feedback.

APPENDIX: CLASSIFICATION OF OBSERVED TOPOLOGIES

In their paper on kinetoplast topology, Chen *et al.* [26] report a scanning electron microscopy (SEM) observation of various catenane structures and use that to refine their estimates. Here, in Fig. 6, we report the zoo of observed topologies, as well as one structure consistent with a catenane of maxicircles and several minicircles.

For each topology predicted from combinatorics, we calculate a "SPIRaL" classification [12] based on the number of concurrent strands within the pore as the molecule translocates, then draw a barcode based on that numeric classification, and compare nonbananular translocation signals to these codes to ascertain molecular topology. We note that we generated the predicted barcodes before undertaking an analysis of the data. The final trace shown is likely a structure consisting of a maxicircle linked to several minicircles.

Several of the more complex structures predicted by Chen *et al.* [26] were not observed. They are shown in Fig. 7. Depending on the rotational configuration at pore entry, more complex structures may admit multiple SPIRaL classifications. Nonetheless, they were not observed.

^[1] D. Branton, D. W. Deamer, A. Marziali, H. Bayley, S. A. Benner, T. Butler, M. Di Ventra, S. Garaj, A. Hibbs, X. Huang *et al.*, The potential and challenges of nanopore sequencing, Nat. Biotechnol. **26**, 1146 (2008).

^[2] M. Jain, H. E. Olsen, B. Paten, and M. Akeson, The oxford nanopore minION: delivery of nanopore sequencing to the genomics community, Genome Biol. 17, 1 (2016).

^[3] W. Yang, L. Restrepo-Perez, M. Bengtson, S. J. Heerema, A. Birnie, J. Van Der Torre, and C. Dekker, Detection of CRISPR-dCas9 on DNA with solid-state nanopores, Nano Lett. 18, 6469 (2018).

^[4] D. Fologea, B. Ledden, D. S. McNabb, and J. Li, Electrical characterization of protein molecules by a solid-state nanopore, Appl. Phys. Lett. **91**, 053901 (2007).

^[5] S. Matysiak, A. Montesi, M. Pasquali, A. B. Kolomeisky, and C. Clementi, Dynamics of Polymer Translocation through

Nanopores: Theory Meets Experiment, Phys. Rev. Lett. **96**, 118103 (2006).

^[6] K. Chen, I. Jou, N. Ermann, M. Muthukumar, U. F. Keyser, and N. A. Bell, Dynamics of driven polymer transport through a nanopore, Nat. Phys. 17, 1043 (2021).

^[7] B. W. Soh, A. R. Klotz, R. M. Robertson-Anderson, and P. S. Doyle, Long-Lived Self-Entanglements in Ring Polymers, Phys. Rev. Lett. 123, 048002 (2019).

^[8] D. J. Mai, A. B. Marciel, C. E. Sing, and C. M. Schroeder, Topology-controlled relaxation dynamics of single branched polymers, ACS Macro Lett. 4, 446 (2015).

^[9] A. R. Klotz, B. W. Soh, and P. S. Doyle, Motion of Knots in DNA Stretched by Elongational Fields, Phys. Rev. Lett. 120, 188003 (2018).

^[10] Q. Wu, P. M. Rauscher, X. Lang, R. J. Wojtecki, J. J. De Pablo, M. J. Hore, and S. J. Rowan, Poly[n] catenanes:

- Synthesis of molecular interlocked chains, Science **358**, 1434 (2017).
- [11] C. Plesa, D. Verschueren, S. Pud, J. van der Torre, J. W. Ruitenberg, M. J. Witteveen, M. P. Jonsson, A. Y. Grosberg, Y. Rabin, and C. Dekker, Direct observation of DNA knots using a solid-state nanopore, Nat. Nanotechnol. 11, 1093 (2016).
- [12] R. K. Sharma, I. Agrawal, L. Dai, P. S. Doyle, and S. Garaj, Complex DNA knots detected with a nanopore sensor, Nat. Commun. 10, 4473 (2019).
- [13] R. K. Sharma, I. Agrawal, L. Dai, P. Doyle, and S. Garaj, DNA knot malleability in single-digit nanopores, Nano Lett. 21, 3772 (2021).
- [14] M. Caraglio, E. Orlandini, and S. Whittington, Driven translocation of linked ring polymers through a pore, Macromolecules 50, 9437 (2017).
- [15] M. Caraglio, E. Orlandini, and S. G. Whittington, Translocation of links through a pore: effects of link complexity and size, J. Stat. Mech.: Theory Exp. (2020) 043203.
- [16] D. Marenduzzo, C. Micheletti, E. Orlandini, and De Witt Sumners, Topological friction strongly affects viral DNA ejection, Proc. Natl. Acad. Sci. USA 110, 20081 (2013).
- [17] V. Narsimhan, C. B. Renner, and P. S. Doyle, Jamming of knots along a tensioned chain, ACS Macro Lett. 5, 123 (2016).
- [18] A. Rosa, M. Di Ventra, and C. Micheletti, Topological Jamming of Spontaneously Knotted Polyelectrolyte Chains Driven Through a Nanopore, Phys. Rev. Lett. 109, 118301 (2012).
- [19] V. Narsimhan, C. B. Renner, and P. S. Doyle, Translocation dynamics of knotted polymers under a constant or periodic external field, Soft Matter 12, 5041 (2016).
- [20] A. Suma, A. Rosa, and C. Micheletti, Pore translocation of knotted polymer chains: How friction depends on knot complexity, ACS Macro Lett. 4, 1420 (2015).
- [21] T. A. Shapiro and P. T. Englund, The structure and replication of kinetoplast DNA, Annu. Rev. Microbiol. 49, 117 (1995).

- [22] N. R. Sturm and L. Simpson, Kinetoplast DNA minicircles encode guide RNAs for editing of cytochrome oxidase subunit III mRNA, Cell 61, 879 (1990).
- [23] B. L. F. Schamber-Reis, S. Nardelli, C. G. Régis-Silva, P. C. Campos, P. G. Cerqueira, S. A. Lima, G. R. Franco, A. M. Macedo, S. D. J. Pena, C. Cazaux *et al.*, DNA polymerase beta from *Trypanosoma cruzi* is involved in kinetoplast DNA replication and repair of oxidative lesions, Mol. Biochem. Parasitol. 183, 122 (2012).
- [24] A. R. Klotz, B. W. Soh, and P. S. Doyle, Equilibrium structure and deformation response of 2D kinetoplast sheets, Proc. Natl. Acad. Sci. USA 117, 121 (2020).
- [25] B. W. Soh, A. Khorshid, D. Al Sulaiman, and P. S. Doyle, Ionic effects on the equilibrium conformation of catenated DNA networks, Macromolecules **53**, 8502 (2020).
- [26] J. Chen, C. A. Rauch, J. H. White, P. T. Englund, and N. R. Cozzarelli, The topology of the kinetoplast DNA network, Cell 80, 61 (1995).
- [27] H. Kwok, K. Briggs, and V. Tabard-Cossa, Nanopore fabrication by controlled dielectric breakdown, PLoS One 9, e92880 (2014).
- [28] E. Orlandini graciously provided data for the unknot, 2-catenane, linear 3-catenane, and triangular 3-catenane in which each component was 200 beads. The translocation times were 442.3 ± 6.6 , 1118.0 ± 14.3 , 2123.2 ± 27.4 , and 1761.8 ± 42.0 , respectively, in units of the Lennard-Jones time (the bead diameter times the mass over the thermal energy).
- [29] T. Ikonen, A. Bhattacharya, T. Ala-Nissila, and W. Sung, Unifying model of driven polymer translocation, Phys. Rev. E 85, 051803 (2012).
- [30] A. Suma and C. Micheletti, Pore translocation of knotted DNA rings, Proc. Natl. Acad. Sci. USA 114, E2991 (2017).
- [31] K. Hagita, T. Murashima, and N. Sakata, Mathematical classification and rheological properties of ring catenane structures, Macromolecules **55**, 166 (2022).